Wideband Endfire On-Glass Array for 5G Handset Applications

Zhang, Jin; Zhang, Shuai; Pedersen, Gert Frølund

Published in:
2019 IEEE 90th Vehicular Technology Conference (VTC2019-Fall)

DOI (link to publication from Publisher):
10.1109/VTCFall.2019.8891142

Publication date:
2019

Document Version
Accepted author manuscript, peer reviewed version

Wideband Endfire On-Glass Array for 5G Handset Applications

1st Jin Zhang
dept. Electronic Systems
Aalborg University
Aalborg, Denmark
jzhang@es.aau.dk

2nd Shuai Zhang
dept. Electronic Systems
Aalborg University
Aalborg, Denmark
sz@es.aau.dk

3rd Gert Frølund Pedersen
dept. Electronic Systems
Aalborg University
Aalborg, Denmark
gfp@es.aau.dk

***Abstract*—A wideband endfire array considering the glass influence at 28 GHz is proposed in this paper. The array element is a bow-tie slot antenna above a ground plane, which has the endfire radiation pattern. A glass layer, which has the same size as the ground plane, is attached on the front side of the array. A trapezoid slot is made on the edge of the ground plane to compensate the influence of the glass layer. The simulated -10-dB bandwidth is 11.3% from 25 GHz to 28 GHz and -6-dB bandwidth is 30.3% from 21 GHz to 28.5 GHz. The horizontal polarized endfire gain of the 4 element array ranges from 7.08 dBi to 8.36 dBi over the operating band. The array covers from -100° to 100°, when the realized gain is above 0 dBi on the XOY plane.**

***Index Terms*—component, formatting, style, styling, insert**

I. Introduction

Since the 5G band has been applied between 20 GHz to 40 GHz, the design of the 5G antennas in the handset devices becomes a hot research topic. To compensate the high path loss of mm-wave (millimeter wave) and at the same time maintain a good spacial coverage, phased arrays become one of the best candidates [1], [2]. Moreover, endfire arrays are preferred because they can provide higher spacial coverage than the arrays with broadside radiation patterns [3], [4]. In [5] has presented a endfire dipole array with wide scan angle from 25 GHz to 33 GHz. However, in the mm-wave band, the other components in the mobile devices have significant influence on the antenna performance, which should also be considered in the antenna design. Many researches focus on the influence of the metal bezels or the low frequency antennas. In [6] has presented endfire arrays with metallic casing. In [7] has introduced an endfire array with the blocking of the metallic casing, which also works as a low frequency antenna. However, there is not much researches investigating the influence of the screen glass. An on-glass antenna for handsets is presented in [8] at 1.575 GHz and 2.45 GHz. At mm-wave band, the glass is expected to have higher influence to the antennas.

Therefore, to investigate the glass effect on the mm-wave antenna, this paper proposes an array with wideband and endfire radiation patterns for 5G handsets, which is compatible with the glass screen. The paper is organized as follows: Section II introduces the array element design, the glass influences on the radiation patterns with different polarization, the glass influence on the impedance matching, and the effect of the metallic wall; Section III presents the simulations of the 4-element array; And the paper is concluded in Section IV.

This work was supported by the AAU Young Talent Program and in part by the Innovations Fonden Project of RANGE (Corresponding author: Shuai Zhang).

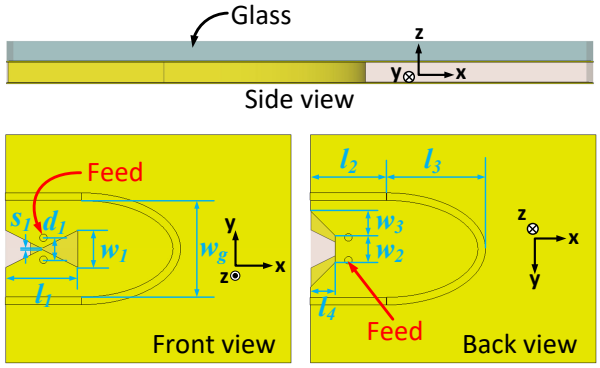

Fig. 1: The configuration of the proposed array element.

TABLE I: The dimensions of the proposed array element. (Units: mm)

s_1	d_1	l_1	l_2	l_3
0.1	1.4	3.8	4	4.8
l_4	w_1	w_2	w_3	w_g
1.3	2	1.4	1.3	5.1

II. Array Element Design and Analysis

A. Array Element Simulation Results

The array element configuration is shown in Fig1. The antenna structure is printed on a PCB with thickness 0.508 mm. The substrate is Rogers RO4350B with $\epsilon_r = 3.66$ and $tan\delta = 0.0037$. The front side of this PCB is attached with a glass layer, which has the thickness of 0.5 mm. Both sides of the PCB is covered by copper. A bow-tie shaped slot is etched on the front side, which generates the endfire horizontal polarized radiation. The trapezoid slot on the back side of the PCB is for adjusting the beam direction, which is affected

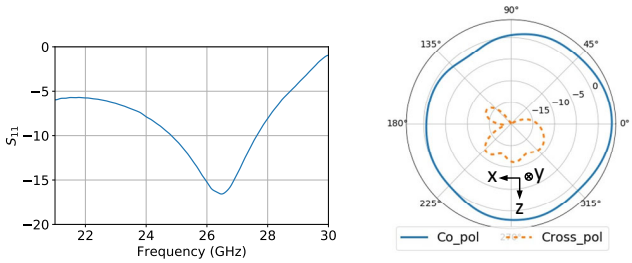

(a) (b)

Fig. 2: The simulation results of the array element. (a) S_{11}, (b) The radiation patterns at 26 GHz.

by the glass. The clearance on the back side equals to the height of the trapezoid slot, which is 1.3 mm. The antenna is surrounded by a metallic wall, which constructs a cavity behind the antenna. The bottom of this wall has a ellipse shape. The minor axis of the ellipse equals to the distance between the two side walls. The antenna is fed by one of the metallic vias next to the slot. The impedance matching is affected by the value of the major axis of the ellipse due to the different reflection from the cavity. All the dimensions are listed in Table.I.

The array element is simulated firstly on a small ground plane, where the size is $15\ mm \times 12\ mm$. The simulation results are shown in Fig.2. Fig.2a is the reflection coefficients and Fig.2b is the radiation patterns of the co-polarization and the cross-polarization at 26 GHz. The simulated realized gain is 3.2 dBi. The backward radiation (+x direction) looks high in Fig.2b because the ground plane size is too small. On the other hand, the wide beamwidth is an advantage because the spatial coverage will also be high, as a result.

B. The Glass Influence on the Radiation Patterns with Different Polarization

For low frequency antennas, the effect of the glass is not significant because the thickness of the glass is very small comparing with the wavelength. However, in mm-wave band, the thickness of the glass is becoming comparable with the wavelength, which brings some effects on the antennas: the loss when microwave penetrates the glass; the blocking to the radiation patterns; the propagating surface wave on the glass; and the changing of impedance matching. First of all, we will focus on the surface wave.

The surface wave becomes stronger when the screen size becomes bigger, which, as a result, will distort the radiation patterns. However, intensity of the surface wave is related to the antenna polarization. The proposed array element is a horizontally polarized antenna, so another vertically polarized antenna is made for comparison. In Fig.3a, a monopole antenna with a reflector is made as a endfire vertically polarized antenna. Both the proposed antenna and the monopole antenna are simulated at 28 GHz on a big ground plane with or without the glass. The size of the ground plane and the glass is $110\ mm \times 60\ mm$. Fig.3b shows the vertically polarized

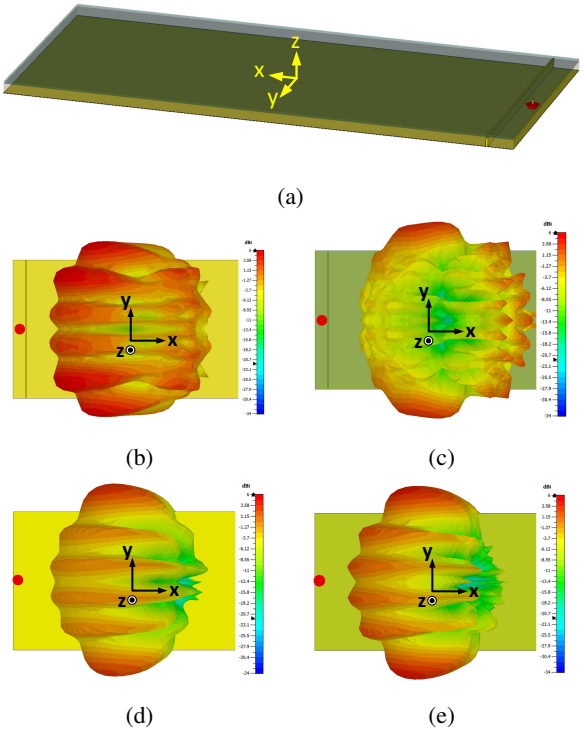

Fig. 3: The glass influence on the antennas with different polarization. (a) The simulation model of the monopole antenna, (b) Vertically polarized antenna without glass, (c) Vertically polarized antenna with glass, (d) Horizontally polarized antenna without glass, (e) Horizontally polarized antenna with glass.

radiation pattern of the monopole antenna without glass and Fig.3d shows the horizontally polarized radiation pattern of the proposed antenna without glass. Both radiation patterns are endfire. The gain of the vertical antenna is higher due to better impedance matching. The ripples are caused by the surface wave propagating on y-axis direction, which will be canceled out between the array elements. Fig.3c shows radiation pattern of the monopole antenna with glass. Because of strong surface current stimulated on the glass, more ripples are observed and the radiation pattern tilted to +x direction. However, the radiation pattern of the proposed antenna with glass, as shown in Fig.3e, does not change too much comparing with Fig.3d. Because the vertically polarized antenna will stimulate much higher surface wave than the horizontal polarized antenna and the surface wave will be enhanced by the glass, the horizontal polarized antenna is less influenced and will be more compatible with the glass.

C. The Glass Influence on Impedance Matching

The glass has significant influence on the impedance matching of the antenna. Therefore, if the antenna is designed without considering glass, the impedance matching will be much different in the real scenario. On the other hand, the glass influence can be considered in the antenna design and

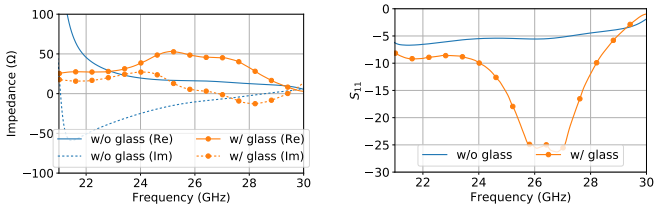

(a) (b)

Fig. 4: The glass influence on impedance matching. (a) Impedance, (b) S_{11}.

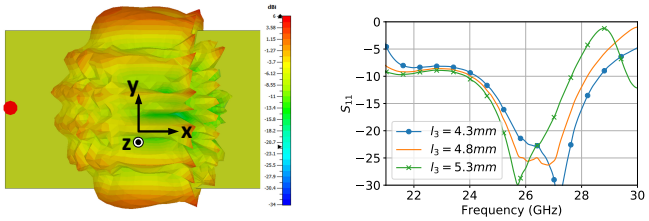

(a) (b)

Fig. 5: The effect of the metallic wall. (a) The radiation pattern without the metallic wall, (b) The S_{11} with different value of l_3.

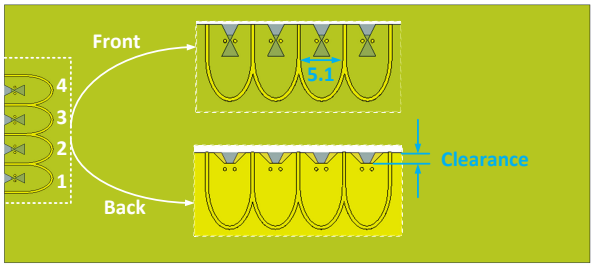

Fig. 6: The configuration of the 4-element array.

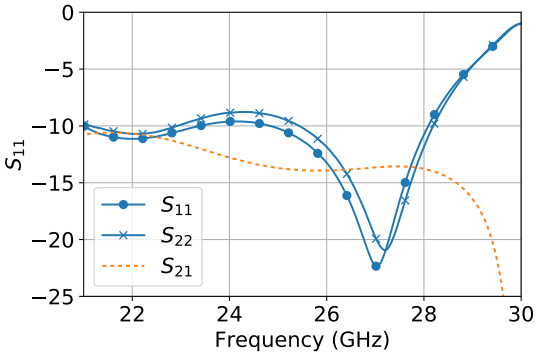

Fig. 7: The simulated S-parameters of the first and second array elements.

good impedance matching is reached with the glass. Fig.4a is showing the simulated impedance of the proposed antenna with or without the glass. When the antenna is not attached on the glass, the resonant frequency is about 21 GHz and the real part of the impedance is high. When the antenna is attached with the glass, the real part of the impedance decreases and two close resonances are observed at about 25 GHz and 27 GHz, which also increase the bandwidth. Fig.4b shows the S_{11} of the proposed antenna with and without glass. The -10-dB bandwidth is from 24 GHz to 28 GHz and the S_{11} from 21 GHz to 24 GHz is still lower than -6 dB.

D. The Effect of the Metallic Wall

The metallic wall surrounding the antenna can effectively stop the surface current propagating in the substrate of the PCB, and as a consequence, reduce the unwanted radiation from the surface wave. Fig.5a shows the radiation patterns of the proposed antenna without the metallic wall. Comparing with Fig.3e, the radiation pattern in Fig.5a has lower endfire gain and more ripples. The shape of the metallic wall also affect the impedance matching. Fig.5b shows the impedance matching of the proposed antenna with different value of the major axis (l_3) of the ellipse increases. The operating frequency decreases as l_3 increasing. In practice, the metallic wall can be replaced by a group of metallic vias.

III. The Simulations of the 4-Element Array

The configuration of the 4-element array is shown in Fig.6. The element distance is 5.1 mm, which is half wavelength of 28 GHz. The clearance on the back is 1.3 mm. Fig.7 presents the reflection coefficients and the mutual coupling of the first and the second array elements. The -10-dB bandwidth is 11.3% from 25 GHz to 28 GHz and the -6-dB bandwidth is 30.3% from 21 GHz to 28.5 GHz. The mutual coupling is lower than -10 dB in the whole operating band. Fig.8 shows the co-polarization and cross-polarization radiation patterns of the second array element from 25 GHz to 28 GHz. The realized gain of the horizontal polarization is ranging from 1.45 dBi to 2.56 dBi. Fig.9 shows the beam scanning patterns on the XOY plane at 27 GHz. The realized gain ranges from 7.08 dBi to 8.36 dBi. The array has a wide coverage from $-100°$ to $100°$, when the realized gain is above 0 dBi.

IV. Conclusion

This paper proposes a wideband endfire on-glass array for 5G handsets. The -10-dB bandwidth is 11.3% from 25 GHz to 28 GHz and the -6-dB bandwidth is 30.3% from 21 GHz to 28.5 GHz. The realized gain ranges from 7.08 dBi to 8.36 dBi at 27 GHz. The glass influences on the radiation patterns and the impedance matching are discussed. The simulations show good performance of the proposed array.

References

[1] W. Hong, K. Baek, and S. Ko, "Millimeter-wave 5g antennas for smartphones: Overview and experimental demonstration," *IEEE Transactions on Antennas and Propagation*, vol. 65, no. 12, pp. 6250–6261, Dec 2017.

[2] J. G. Andrews, S. Buzzi, W. Choi, S. V. Hanly, A. Lozano, A. C. K. Soong, and J. C. Zhang, "What will 5g be?" *IEEE Journal on Selected Areas in Communications*, vol. 32, no. 6, pp. 1065–1082, June 2014.

[3] J. Helander, K. Zhao, Z. Ying, and D. Sjberg, "Performance analysis of millimeter-wave phased array antennas in cellular handsets," *IEEE Antennas and Wireless Propagation Letters*, vol. 15, pp. 504–507, 2016.

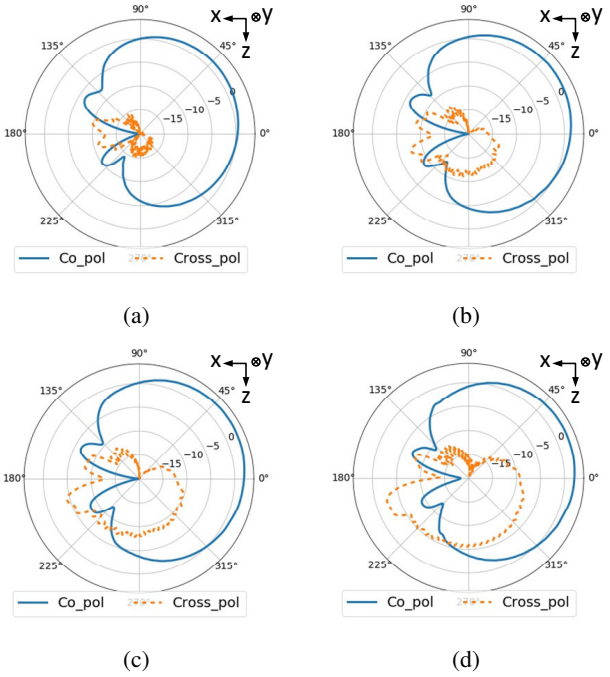

Fig. 8: The simulated radiation patterns of the second array element. (a) 25 GHz, (b) 26 GHz, (c) 27 GHz, (d) 28 GHz.

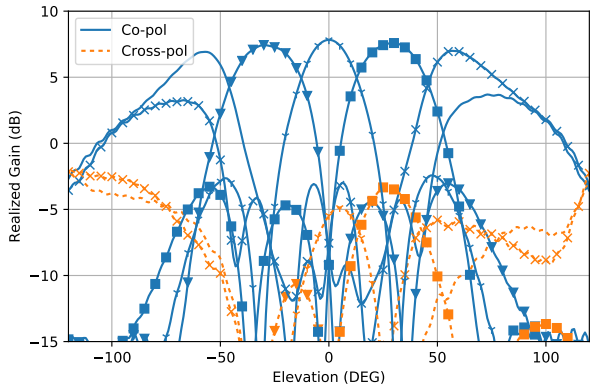

Fig. 9: The beam scanning patterns on the XOY plane at 27 GHz.

[4] K. Zhao, S. Zhang, Z. Ho, O. Zander, T. Bolin, Z. Ying, and G. F. Pedersen, "Spherical coverage characterization of 5g millimeter wave user equipment with 3gpp specifications," *IEEE Access*, vol. 7, pp. 4442–4452, 2019.

[5] I. Syrytsin, S. Zhang, G. F. Pedersen, and A. S. Morris, "Compact quad-mode planar phased array with wideband for 5g mobile terminals," *IEEE Transactions on Antennas and Propagation*, vol. 66, no. 9, pp. 4648–4657, Sep. 2018.

[6] B. Yu, K. Yang, C. Sim, and G. Yang, "A novel 28 ghz beam steering array for 5g mobile device with metallic casing application," *IEEE Transactions on Antennas and Propagation*, vol. 66, no. 1, pp. 462–466, Jan 2018.

[7] R. Rodriguez-Cano, S. Zhang, K. Zhao, and G. Pedersen, "Reduction of main beam-blockage in an integrated 5g array with a metal-frame antenna," *IEEE Transactions on Antennas and Propagations*, 2019.

[8] C. Lin, L. Lai, K. Tiong, and G. Chen, "A novel on-glass antenna for mobile handset applications," in *2012 International Symposium on Computer, Consumer and Control*, June 2012, pp. 236–239.